

## Size distribution dependence of the dielectric function of Si quantum dots described by a modified Maxwell-Garnett formulation

A.-S. Keita\* and A. En Naciri

*Laboratoire de Physique des Milieux Denses (LPM), Université Paul Verlaine-Metz, 1 Bd Arago, 57070 Metz Technopôle, France*  
(Received 31 March 2011; revised manuscript received 30 May 2011; published 19 September 2011)

Numerical inversion of effective medium equations used in ellipsometry data analysis are carried out, without using any parameterized dispersion formula, in order to investigate on the influence of size distribution (SD) on the dielectric properties of silicon quantum dots (Si QDs) within a silica matrix over the energy range [0.65–6.5 eV]. To do so the dielectric function (DF) of the whole inhomogeneous layer is properly determined, and then a modified version of the Maxwell-Garnett (MG) formula, which is often used in the ellipsometric modeling of nanoscale Si, is set forth. This formula, which accounts for SD, was formerly introduced by Bányai and Koch. We show that a small change in the size dispersion value may induce a sensitive modification in the line shape of the DF. It is also pointed out that if only the filling factor  $f$  is accounted for as in the classical MG formula this may lead to the overestimation of the amplitude of the DF of the Si nanoclusters. Furthermore the use of  $f$  solely may induce an undervaluation of the optical-gap energy of the Si QDs but also of the broadening and transition energies associated to the  $E_1$ -like and  $E_2$ -like critical points of crystalline Si. Likewise it is shown that SD does have an impact on the static dielectric constant  $\epsilon_0$  at low frequency, contrary to what has been generally supposed. Indeed it is demonstrated that provided that either quantum confinement or surface polarization is considered, then the parameters describing the size dependence of  $\epsilon_0$  at 0.65 eV are subjected to sensitive changes as the size dispersion  $\sigma$  increases.

DOI: [10.1103/PhysRevB.84.125436](https://doi.org/10.1103/PhysRevB.84.125436)

PACS number(s): 78.67.Bf, 78.66.Sq, 77.22.Ch, 07.60.Fs

### I. INTRODUCTION

Silicon is a material of primary interest in microelectronics. For this reason its optical and dielectric properties have been thoroughly determined and mastered since pioneering works were earlier carried out.<sup>1–7</sup> Moreover, the dielectric function (DF) of Si has been parameterized with various dispersion formulas that reproduce the experimental data quite well. Current research focuses on the investigation of the dielectric properties of nanometer-sized silicon embedded within silicon-rich silicon oxide (SRSO) films. The objectives of such investigations lie in potential applications for the building of optoelectronic devices.<sup>8</sup> When it comes to studying silicon in a reduced dimension, some uncertainties arise about the accurate evolution of the DF line shape. These observations originate from the different results deduced from ellipsometry analysis. On one hand this incertitude is certainly owed to the mixture models generally used to describe the dielectric properties of the nanoparticles. On the other hand these uncertainties may emanate from the use of a single average size considered in the modeling while passing over the corresponding size dispersion commonly observed in Transmission Electron Microscopy (TEM) images.<sup>9–15</sup> Nevertheless most of the previous studies show a redshift of the  $E_2$ -like absorption peak and a decrease in the amplitude of the DF with respect to that of crystalline Si (c-Si). Such behavior of the DF has primarily been attributed to quantum confinement effect (QCE).<sup>9–15</sup>

The complex nature of the investigated media brings about interesting questions concerning the physical models used to extract the local dielectric properties of the silicon quantum dots (Si QDs). These properties are embedded in the optical response of the composite film formed by the nanoclusters and dielectric matrix. Maxwell-Garnett (MG) theory is one of the most used effective medium approximations. An MG model enables the determination of the dielectric properties of

heterogeneous films.<sup>16,17</sup> Its conditions of applications require well-separated spherical inclusions with a low volume fraction in order to satisfy the dipolar approximation. The effective dielectric function (EDF)  $\tilde{\epsilon}_{\text{eff}}(\omega)$  of a composite material is defined as the averaged DF of that entire medium, here the whole SRSO layer. It takes into account the contributions of the various pure phases in it.<sup>16,17</sup> Thereafter we will consider only a two-phase medium composed of the QDs and the matrix. The EDF inherently contains information about the inhomogeneous film properties such as the volume fraction of the inclusions embedded within the layer and the signature of any crystalline phase.<sup>10–12,14</sup>

The various deposition techniques [plasma-enhanced chemical vapor deposition (PECVD),<sup>9</sup> ion implantation,<sup>10</sup> evaporation,<sup>11–13</sup> co-sputtering,<sup>14,15</sup> currently used do not enable the elaboration of Si QDs rigorously uniform in size. Hence such SRSO films represent, on a microscopic view, disordered media. Consequently, size dispersion is always present no matter how small it is. Even though a Gaussian function<sup>18,19</sup> has been often applied to describe the size distribution (SD) of semiconductor QDs embedded within a dielectric matrix, many experiments show that the SD is rather of lognormal type.<sup>11–13,20,21</sup> This latter kind of SD has to be preferred to the former one because it represents a more physical description of the QDs ensemble, specifically for very small size (when radius  $R \rightarrow 0$ ). Additionally a lognormal SD is more frequently encountered in systems like SRSO films that have been submitted to high-temperature annealing. Subsequently to such a thermal process, the Si QDs lose the memory of their specific initial germination conditions and undergo a random nucleation and growth in a homogenous medium.<sup>20,21</sup> However, an experimental demonstration of the effect of SD by using spectroscopic ellipsometry is unavailable in the literature.

Therefore, a matter arises regarding the latter subject. How can SD influence the dielectric properties of Si QDs and their associated optical transitions? By attempting to answer that issue, we are putting forward in this paper an approach that allows the modeling of the dielectric properties of semiconductor QDs dispersed in thin dielectric films. Such method takes into account their SD. This work is based on, first, the determination of the EDF from experimental spectra. Subsequently, numerical inversions are performed by using effective medium equations. The outline of our study is divided into three parts. In Sec. II we introduce the modified Maxwell-Garnett (MMG) formula<sup>20,21</sup> that is to be used in the calculations. In Sec. III we present the results obtained by considering the size dispersion effect as given in the MMG formula. We also provide some comparisons with the main works available in the literature. Finally in Sec. IV we discuss the influence of quantum confinement and surface polarization on the SD-dependent static dielectric constant at 0.65 eV.

## II. MMG EXPRESSION AND NUMERICAL INVERSION

Let a host medium of dielectric constant  $\varepsilon_2$  contain spherical QDs of the same size and be characterized by  $\varepsilon_1$ . It is assumed that the QDs are homogeneously distributed in the medium. We presume that the concentration of the QDs is low and their radii are smaller than the distance between each of them. Thus such collection of QDs can be assimilated to electric dipoles. As a result it is possible to show that the effective dielectric constant  $\varepsilon_{\text{eff}}$  of such a system is expressed as<sup>16,17,22</sup>

$$\varepsilon_{\text{eff}} = \frac{1 + \frac{8\pi}{3\varepsilon_2} \cdot n \cdot \kappa}{1 - \frac{4\pi}{3\varepsilon_2} \cdot n \cdot \kappa}, \quad (1)$$

where the number of QDs per unit volume (concentration)  $n$  is related to their volume fraction  $f$  through the expression  $f = \frac{4\pi R^3}{3} \cdot n$ , and the polarizability  $\kappa$  of the QDs is defined as

$$\kappa = \frac{\varepsilon_1 - 1}{\frac{\varepsilon_1}{\varepsilon_2} + 2} \cdot \varepsilon_2 \cdot R^3. \quad (2)$$

The former equations lead to the well-known MG formula<sup>17</sup>

$$\frac{\varepsilon_{\text{eff}} - \varepsilon_2}{\varepsilon_{\text{eff}} + 2 \cdot \varepsilon_2} = f \cdot \frac{\varepsilon_1 - \varepsilon_2}{\varepsilon_1 + 2 \cdot \varepsilon_2}. \quad (3)$$

At this stage it can be remarked that in the MG model the information about the average size of the inclusions is implicitly contained in the value of the volume fraction  $f$  and the polarizability  $\kappa$  as far as a system of identical QDs and homogeneously distributed inside a host material is supposed.

Bányai and Koch<sup>22</sup> previously suggested that if a system contains dots of different radii with a given SD  $P(R)$ , then the expression of the polarizability  $\kappa$  should be revised in order to take into account the effect of that SD. Thereby the quantity  $\kappa$  is weighted by  $P(R)$  and substituted in Eqs. (1) and (2) by an average polarizability  $\bar{\kappa}$  formulated as

$$\bar{\kappa} = \int_0^\infty dR \kappa \cdot P(R). \quad (4)$$

Hence the classical MG formula should be replaced by an MMG formula [Eq. (5)] for absorbing materials,

$$\frac{\tilde{\varepsilon}_{\text{eff}}(\omega) - 1}{\tilde{\varepsilon}_{\text{eff}}(\omega) + 2} = f \cdot \int_0^\infty dR (R/\bar{R})^3 \cdot P(R) \cdot \frac{\tilde{\varepsilon}_{\text{QDs}}(\omega, R) - 1}{\tilde{\varepsilon}_{\text{QDs}}(\omega, R) + 2}, \quad (5)$$

where the host material is void ( $\varepsilon_2 = 1$ ).<sup>22</sup>

We have applied this formula to the case of Si QDs embedded within a silica matrix and this MMG formula is established by the equation

$$\frac{\tilde{\varepsilon}_{\text{eff}}(\omega) - \tilde{\varepsilon}_{\text{SiO}_2}(\omega)}{\tilde{\varepsilon}_{\text{eff}}(\omega) + 2 \cdot \tilde{\varepsilon}_{\text{SiO}_2}(\omega)} = f \cdot \int_{R_{\text{min}}}^{R_{\text{max}}} dR (R/\bar{R})^3 \cdot P(R) \times \frac{\tilde{\varepsilon}_{\text{QDs}}(\omega, R) - \tilde{\varepsilon}_{\text{SiO}_2}(\omega)}{\tilde{\varepsilon}_{\text{QDs}}(\omega, R) + 2 \cdot \tilde{\varepsilon}_{\text{SiO}_2}(\omega)}, \quad (6)$$

where  $\tilde{\varepsilon}_{\text{eff}}(\omega)$  is the EDF of the whole composite layer;  $\tilde{\varepsilon}_{\text{SiO}_2}(\omega)$  is the DF of the silica matrix; and  $\tilde{\varepsilon}_{\text{QDs}}(\omega, R) = \varepsilon_r + i\varepsilon_i$  is the DF of the Si QDs with a given radius  $R$  (in nm) and  $\omega$  is the photon energy (in eV). In Eq. (6)  $P(R)$  is the QD SD that has been chosen here to be a normalized lognormal SD which is defined as

$$P(R) = \frac{1}{R \cdot \sqrt{2\pi} \cdot \text{Log}(\sigma)} \times \text{Exp}\left(-\left(\frac{\text{Log}[R/\bar{R}]}{\sqrt{2} \cdot \text{Log}(\sigma)}\right)^2\right). \quad (7)$$

In Eq. (7) the standard deviation (that we call size dispersion further in the text)  $\sigma$  ( $\sigma > 1$ ) is expressed as

$$\text{Log}(\sigma) = \left[ \frac{\sum_j N_j \cdot (\text{Log}(R_j) - \text{Log}(\bar{R}))^2}{\sum_j N_j} \right]^{1/2}, \quad (8)$$

where  $N_j$  is the number of inclusions with a radius equal to  $R_j$ .  $R_{\text{min}}$  and  $R_{\text{max}}$  represent the lower and upper bounds in which the SD  $P(R)$  evolves.

It is noteworthy that for disordered systems the ensemble-averaged EDF can also be determined from first principles in terms of  $n$ -particle distribution functions.<sup>23</sup> Hence, MG approximation can be considered as a particular case when dealing with two-particle spherical distribution. Although it was shown earlier that both size and shape distributions can affect both the EDF of the system<sup>24</sup> and the DF of the embedded nanoclusters, the MMG formulation is restricted in this work to the case of QDs with a spherical shape, which models the best shape describing the QDs in our samples. Nonetheless, the MMG model may have several extensions among which the potential application to systems, (i) with a bimodal SD of the QDs; (ii) with an SD of ellipsoidal QDs using the generalized MG theory;<sup>25</sup> and (iii) with two different kinds of shape distributions, *e.g.*, both ellipsoidal and spherical QDs with diverse sizes. Practically,  $P(R)$ ,  $R_{\text{min}}$ , and  $R_{\text{max}}$  should be assessed by TEM observation which, however, currently has a detection limit of 1 nm in radius. The EDF  $\tilde{\varepsilon}_{\text{eff}}(\omega)$  of the SRSO layer can be obtained with a good precision from ellipsometry modeling using either dispersion formula<sup>9,10,13</sup>

or wavelength-by-wavelength numerical inversion.<sup>11,12,14</sup> An assumption is usually made that  $\tilde{\epsilon}_{\text{SiO}_2}(\omega)$  may not be radically changed from the data provided in the literature, even though in strict reality there are interactions between the matrix and the QDs, which should lead to slight deviations of  $\tilde{\epsilon}_{\text{SiO}_2}(\omega)$  from the tabulated values.<sup>11,12</sup> An explicit analytical dependence of  $\tilde{\epsilon}_{\text{QDs}}(\omega)$  with the QDs' size is not known to date. Thereafter, we will presume that such dependence of  $\tilde{\epsilon}_{\text{QDs}}(\omega)$  with size in Eq. (1) may be implicitly contained in the characteristic parameters (transition energy, amplitude, and broadening) for nanocrystalline materials as described elsewhere.<sup>26–31</sup> By assuming that in Eq. (6)  $\tilde{\epsilon}_{\text{QDs}}(\omega)$  is the only unknown, we can numerically solve that equation and find the energy dependence of the DF of the Si nanoclusters.

### III. SIZE DISPERSION EFFECT ON THE LINE SHAPE OF THE OPTICAL FUNCTION OF THE Si QDs

Pavesi *et al.*<sup>8</sup> employed an MG relationship in order to evaluate the effective refractive index  $n_{\text{eff}}$  of their SRSO films in which were embedded Si nanocrystals (Si-ncs) with an average diameter of 3 nm and a volume fraction  $f = 28\%$ . In that work it was shown that a decrease of the optical filling-factor value, implicitly connected to the SD of the nanocrystals, led to a perceptible variation—around 10%—of  $n_{\text{eff}}$  in the nanocrystalline region. Hence in our case, a careful analysis of this EDF should be a necessary investigation preliminarily to determine the dielectric properties of the Si QDs. Such investigation has not always been reported in preceding works.<sup>9,10,13,14</sup> Figure 1 shows the EDF of an SRSO layer elaborated by ion implantation. The estimated volume fraction of Si QDs was 5.0%. The latter value was deduced from a model presented in a previous work.<sup>32</sup> This modeled EDF  $\tilde{\epsilon}_{\text{mod}}$  was obtained from the fit of the experimental ellipsometric data using wavelength-by-wavelength numerical inversion. Besides, the same figure presents for comparison the DF of silica  $\tilde{\epsilon}_{\text{SiO}_2}$  and a calculated EDF  $\tilde{\epsilon}_{\text{cal}}$  corresponding to an MG mixture between a host medium of silica ( $f = 95\%$ ) and inclusions of crystalline Si ( $f = 5\%$ ). The quantities  $\tilde{\epsilon}_{\text{SiO}_2}$  and  $\tilde{\epsilon}_{\text{c-Si}}$  are known values from the literature.<sup>33</sup>

In Fig. 1 it is seen that the amplitude of the real part of  $\tilde{\epsilon}_{\text{mod}}$  and  $\tilde{\epsilon}_{\text{cal}}$  are much higher than that of silica. Moreover, the absorption onset starts at nearly 2 eV on the imaginary part of  $\tilde{\epsilon}_{\text{SiO}_2}$  and  $\tilde{\epsilon}_{\text{cal}}$ . All these points are features of the presence in the SiO<sub>2</sub> matrix of a silicon excess, which is under two distinct forms: nanocrystalline Si (for the line shape of  $\tilde{\epsilon}_{\text{mod}}$ ) and crystalline Si (for the line shape of  $\tilde{\epsilon}_{\text{cal}}$ ). It is noteworthy that, from the examination of  $\tilde{\epsilon}_{\text{cal}}$ , the presence of some structures, indicated by the vertical arrows in this figure, is observed. These structures stem from the signature of  $E_1$  (at 3.4 eV),  $E_2$  (at 4.26 eV), and  $E'_1$  (at 5.5 eV) transitions in the imaginary DF of c-Si. In the case of  $\tilde{\epsilon}_{\text{mod}}$  no prominent signature of either the  $E_1$  transition or the  $E'_1$  one exists. The same observation seems to be valid when analyzing the EDF of systems with a higher volume fraction ( $f = 29\%$ ) of Si QDs, such as in Refs. 11 and 12. This observation can be interpreted as a consequence of the reduction in the size of the Si inclusions and/or the formation of a suboxide shell around the Si QD structure.

In all of the results subsequently presented the size dispersion  $\sigma$  ranges between 1.05 and 1.40, while the average

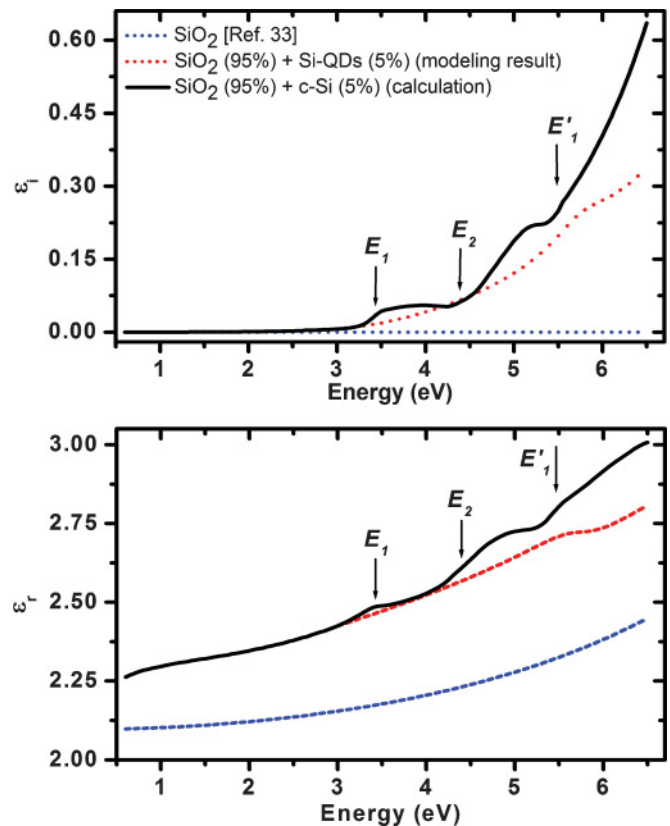


FIG. 1. (Color online) DF of (a) SiO<sub>2</sub> extracted from the literature (dash-dot line); (b) the effective medium of a calculated MG mixture between a host medium of silica and crystalline Si inclusions in a proportion of 95% and 5% volume fractions, respectively (solid line); (c) the effective medium of the modeled SRSO layer containing a volume fraction of nanocrystalline Si QDs evaluated to 5.0% as estimated in Ref. 32 (dash line).

radius of the Si QDs is set constant to  $\bar{R} = 1.5$  nm. The values of  $R_{\text{min}}$  and  $R_{\text{max}}$  move between 0.5 and 3.0 nm, respectively. The volume fraction of the Si QDs is constant and equal to 5.04%. The curves in Fig. 2 display the probability density of different lognormal SDs obtained from Eq. (2) by varying the values of the standard deviation  $\sigma$ . As  $\sigma$  increases, a sprawl of the SD toward both larger and smaller radii is observed. Indeed a slight elevation of  $\sigma$  from 1.05 to 1.15 leads to a more than double radii range. At the same time the probability density maximum is slightly skewed (from 1.50 to 1.34) toward the smallest radii (as is observed in the inset of Fig. 2 and also in Table I). Thus for  $\sigma$  values higher than 1.15, most of the QDs have a size smaller than the average size of  $\bar{R} = 1.5$  nm. The vertical arrow in Fig. 2 indicates the size (radius) detection limit of the QDs, which is equal to 1 nm generally for the actual TEM instruments. It is striking that as  $\sigma$  goes up the contribution of QDs with a radius less than 1 nm cannot be neglected especially as the quantum confinement is more important for such sizes.

Figure 3 shows the imaginary DFs obtained for Si QDs whose diameters range between 3.0 and 4.7 nm. The data were extracted from literature. Losurdo *et al.*<sup>9</sup> synthesized by PECVD nanocrystalline Si ( $f = 38\%$  in an hydrogenated amorphous Si matrix) of approximately 3 nm in diameter with a size

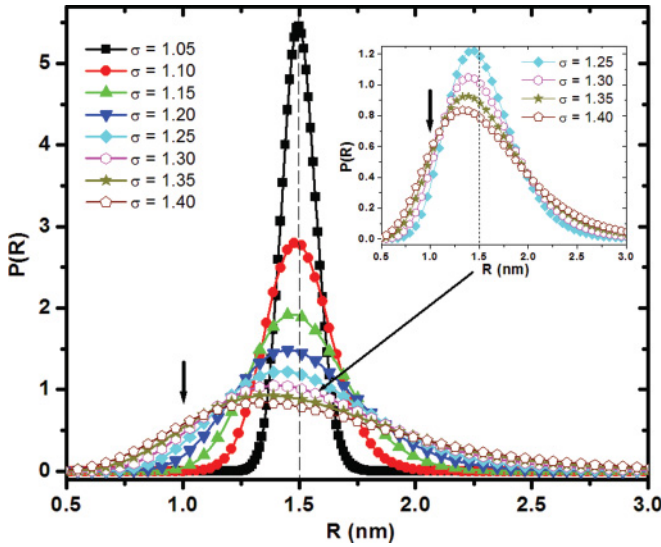


FIG. 2. (Color online) Probability densities  $P(R)$  of some lognormal SDs obtained by varying the values of the standard deviation  $\sigma$  from 1.05 to 1.40. The average radius is  $\bar{R} = 1.5$  nm. The inset shows the distribution  $P(R)$  associated to  $\sigma$  values between 1.25 and 1.40. The detection limit of the conventional TEM instruments—generally around 1 nm in radius—is indicated by a vertical arrow.

dispersion in the range  $1.20 \leq \sigma \leq 1.30$  as estimated from the histogram of the TEM image. Furthermore, Ding *et al.*<sup>10</sup> used MG theory in order to derive the DF of ion-implanted Si-ncs. The latter Si-ncs ( $f = 17\%$  in an  $\text{SiO}_2$  matrix) had an average size of 4.6 nm with a given size dispersion that was not specified. Gallas *et al.*<sup>11,12</sup> employed Bruggeman Effective Medium Approximation (BEMA) for the characterization of Si-ncs ( $f = 29\%$ ) within evaporated SRSO layers. The size standard deviation was estimated to range between 1.15 and 1.20 from the histogram of the TEM image. En Naciri *et al.*<sup>32</sup> elaborated ( $f = 5.04\%$ ) by ion-implantation within silica. The size dispersion was evaluated to be approximately 1.20. More recently Alonso *et al.*<sup>14</sup> also modeled nanocrystalline Si of average sizes comprised between 4.2 ( $f = 18\%$ ) and 4.7 nm ( $f = 20\%$ ) embedded in a sputter-deposited  $\text{SiO}_2$  matrix. In their work the DF of the Si nanoclusters was extracted using BEMA as well. The corresponding size dispersions are in the range  $1.20 \leq \sigma \leq 1.30$  as evaluated from the histogram of

TABLE I. Variation with size dispersion  $\sigma$  of different parameters characterizing the line shape of the Si nanoclusters.  $C$  is taken as the full width at half maximum of the imaginary DF. The significance of the other parameters is given in the text.

$\bar{R}$ (nm)	$f$ (%)	$\sigma$	$R_0$ (nm)	$A$	$C$ (eV)	$E$ (eV)	$E^{04}$ (eV)	$\varepsilon_0$
		1.00	1.50	37.5	1.55	4.15	2.27	9.00
		1.05	1.50	35.4	1.65	4.20	2.28	8.85
		1.10	1.49	30.9	1.75	4.30	2.30	8.49
		1.15	1.47	24.9	1.85	4.50	2.37	7.90
1.50	5.04	1.20	1.45	20.2	2.07	4.65	2.40	7.32
		1.25	1.43	16.4	2.55	4.85	2.45	6.71
		1.30	1.40	14.0	—	5.00	2.52	6.23
		1.35	1.37	11.5	—	5.15	2.57	5.65
		1.40	1.34	9.46	—	5.30	2.61	5.07

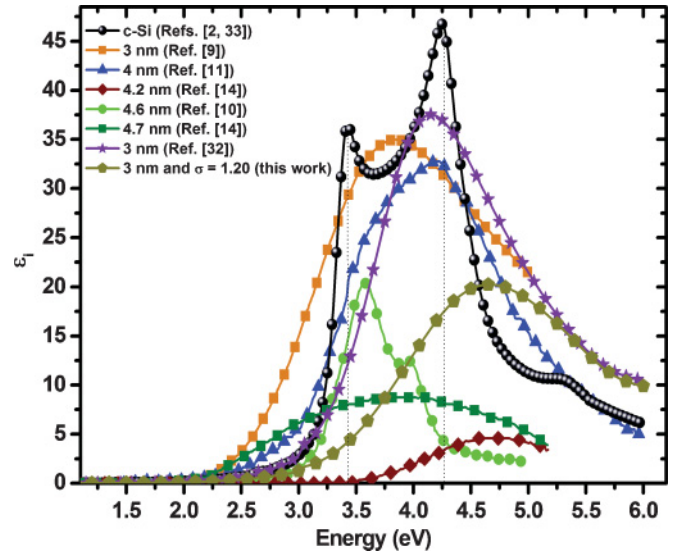


FIG. 3. (Color online) Comparison between some of the various imaginary DFs obtained in the literature for Si QDs of specified average size (diameter). The imaginary DF of Si QDs that takes into account a size dispersion  $\sigma = 1.20$ , deduced from this work, is also depicted. The imaginary DF of c-Si is also plotted for comparison. The position of the  $E_1$  (3.4 eV) and  $E_2$  (4.26 eV) transitions are evidenced by vertical dotted lines.

the TEM image in Refs. 14 and 15. The different features of these referenced optical functions for Si nanoclusters are summarized in Table II.

Regarding the previous DF line shapes of nanocrystalline Si, some similarities between them can be noticed. Indeed there is (i) a decrease of the amplitude with respect to crystalline Si; (ii) a red shift of the main transition energy as compared to  $E_2$ ; and (iii) a broadening of the optical resonances relatively to the bulk materials. Nonetheless, some quantitative disagreements remain unresolved. As an example Fig. 3 shows a fall of the amplitude of the DF from three nanometer-sized Si QDs to 4.7 nanometer-sized Si QDs, whereas the quantum confinement theory predicts the opposite trend to occur. Thus some hypotheses may be put forward in order to explain such differences. First the deposition and annealing conditions may significantly influence the optical properties of Si QDs. The former elaboration parameters could result, secondly, in silica matrices with different (optical) properties and hence this could affect the local environment of the Si QDs. However, Table II and Fig. 3 show that for rather close values of the filling factor ( $f \approx 18\%$ ) and average radius  $\bar{R} \approx 2.6$  nm, Ding *et al.*<sup>10</sup> and Alonso *et al.*<sup>14</sup> obtained line shapes for the DF that seem radically dissimilar. In both studies an identical silica matrix, whose optical properties were extracted from the literature,<sup>33</sup> was reported. Furthermore, we stress here on the fact that silica is totally transparent in the [0.6–6.5 eV] photon-energy range.<sup>33</sup> Consequently comes into play a third interpretation of such discrepancies, which has to be attributed to the impact of SD in the previous SRSO films as evidenced by the corresponding TEM histograms.

From the perspective of numerical simulations *ab initio* results showed that for embedded QDs (of 1 nm large at least but sufficiently small), both BEMA and MG theory

TABLE II. Description of the different main features related to the dielectric properties of nanocrystalline Si available in the literature. The size standard deviation  $\sigma$  is evaluated from the shape of the SD of the corresponding TEM histogram. In the case of Si QDs, the parameter  $C$  is determined using Lorentzian oscillators in order to make a deconvolution of the DF line shape. The symbol “\*” means that the associated gap energy is actually not the fundamental gap  $E_g$  but the optical gap  $E^{04}$ . As a comparison, the parameters of the line shape of the Si QDs with  $\sigma = 1.20$  are also presented (as obtained in this work). The DF of crystalline, polycrystalline, and amorphous Si are also presented.

Authors	$\bar{R}$ (nm)	$f$ (%)	EMT	DF derivation	Estimated $\sigma$	$A_i$	$C_i$ (eV)	$E_i$ (eV)	$E_g$ (eV)	$\epsilon_r$ at $E = 1$ eV
This work	1.50	5.0	MMG	$\lambda$ -by- $\lambda$ inversion	1.20	20.2	2.07	4.65	2.40*	8.99
Losurdo <i>et al.</i> <sup>9</sup>	1.50	38	BEMA	Forouhi-Bloomer	1.20–1.30	34.0	3.05	3.8	1.97	10.6
						13.2	0.75	3.58	1.97*	12.2
Gallas <i>et al.</i> <sup>11</sup>	2.00	29	BEMA	$\lambda$ -by- $\lambda$ inversion	1.15–1.20	28.2	1.32	4.22		
						0.96	0.58	5.25		
Alonso <i>et al.</i> <sup>14</sup>	2.10	18	BEMA	$\lambda$ -by- $\lambda$ inversion	1.20–1.30	4.73	–	4.70	2.36	4.24
Ding <i>et al.</i> <sup>10</sup>	2.30	17	MG	Forouhi-Bloomer	–	19.8	0.53	3.54	1.74	10.3
						4.99	0.19	3.95		
Alonso <i>et al.</i> <sup>14</sup>	2.35	20	BEMA	$\lambda$ -by- $\lambda$ inversion	1.20 – 1.35	5.98	1.98	3.58	2.09	6.02
						4.61	1.80	4.39		
						24.4	0.24	3.42	1.12	12.4
c-Si <sup>2,33</sup>	–	–	–	–	–	24.6	0.75	3.74		
						32.2	0.44	4.26		
						4.77	1.22	5.39		
						17.3	0.67	3.51	–	–
p-Si <sup>5</sup>	–	–	–	–	–	30.6	1.05	4.11		
						4.44	0.79	5.37		
a-Si <sup>6,33</sup>	–	–	–	–	–	29.9	2.24	3.72	1.39	–

remained valid and led to similar results.<sup>27–29</sup> This remark holds especially when comparing the DFs obtained in the work of Ref. 10, where MG was employed, and the study of Ref. 14, in which BEMA was used. According to the remarks of Weissker *et al.*,<sup>27–29</sup> the deviations observed between these two DFs should not be primarily attributable to the use of either BEMA or MG.

Wood and Ashcroft<sup>34</sup> examined the quantum-size effects in the optical properties of small metallic particles. They observed that the dc electric dipole conductivity (also linked to the DF) is suppressed by a factor  $O(10–100)$  with respect to the bulk value. Moreover, they noted the prominent presence of broadened absorption peaks. Above all they stressed on the fact that in order to make meaningful comparisons between the predictions of the quantum size effect and experiment, the distribution of particle sizes in real systems must be taken into account. In light of these prior results, the same trends can be qualitatively envisaged when characterizing the dielectric properties of a nanocrystalline semiconductor like Si. Besides this, Khurgin *et al.*<sup>35</sup> proceeded to a systematic study of the size dependence of the photoluminescence (PL) spectra of Si-ncs in an SiO<sub>2</sub> matrix. They showed that when size dispersion rather than specific mean size is taken account, then the confinement model seems to explain reasonably well the experimental PL. On that account we can hypothesize on a possible impact of SD on the absorption process of Si QDs.

Figure 4 plots the evolution of the real and imaginary parts of the DF of an ensemble of Si QDs with an average radius of 1.5 nm and a corresponding size dispersion  $\sigma$ . The results in Fig. 4 were determined from the numerical inversion of Eq. (6), without using any fitting quantity. The evaluation of the second

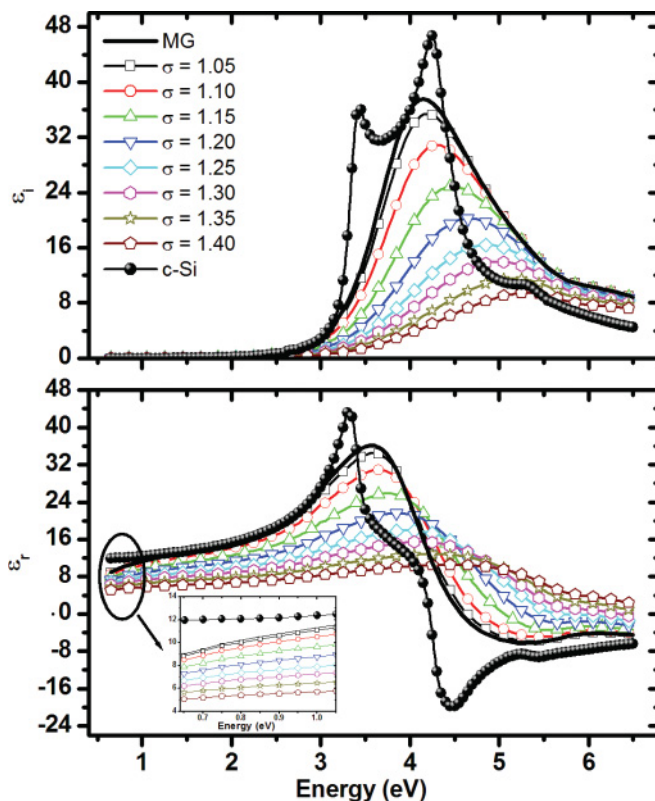


FIG. 4. (Color online) Optical properties of the Si nanoclusters obtained with MMG formula for various values (from 1.05 to 1.40) of the size dispersion  $\sigma$ . The DF of c-Si is also plotted. The inset shows the evolution of the real DF in the range [0.65–1.05 eV].

derivative of  $\varepsilon_i$  reveals the presence of a single peak only that may come from the  $E_2$  one of c-Si. It is noticeable that Ding *et al.*<sup>10</sup> and Zhang *et al.*<sup>13</sup> clearly observed the presence of the  $E_1$ -like and  $E_2$ -like peaks. In the previous reports the DF was evaluated by employing dispersion formulas with more than 16 fitted parameters, contrary to the inversion method used in this work. Next we are to give a close look over the variations with  $\sigma$  of the characteristic parameters of the DF line shape by comparing our results with those obtained in former experimental and theoretical research. Five interesting points arise from the observation of the line shape of  $\varepsilon_i$  in this figure.

First we concentrate on the quantity  $A$  of  $\varepsilon_i$ , which is linearly connected to the oscillator strength and measures the probability of a quantum mechanical transition.<sup>36,37</sup> The outcomes of our calculations, presented in Fig. 1, depict a dramatic fall of the amplitude  $A$  of  $\varepsilon_i$  as the size dispersion rises: indeed, an augmentation of  $\sigma$  of 20% divides the value of  $A$  by more than 1.85. *Ab initio* simulations performed on embedded Si-ncs pointed out a reduction of the DF amplitude with a reduction of their size.<sup>27-31</sup> According to such research the transition probabilities of the lowest transitions remain small. Ding *et al.*<sup>10</sup> found that for Si QDs of roughly 4.6 nm, the DF line shape is marked by the domination of an  $E_1$ -like transition, whereas the contribution of the  $E_2$  one is much weaker (see Table II). On another side the  $E_1$ -like participation on the dielectric behavior seems to be a good deal lower, according to Alonso *et al.*<sup>14</sup> Moreover, in the work of Ref. 14 the magnitude of the imaginary DF of approximately 4.7 nm diameter Si-ncs is around  $A \approx 8.9$ . This value seems to be significantly reduced as compared to the result of Ref. 10, where  $A \approx 19.8$  for nearly 4.6 nm diameter Si-ncs. Likewise according to Ref. 14, Si QDs with an average diameter of 4.2 nm have  $A \approx 4.7$  whereas it is importantly increased up to  $A \approx 28.2$ , as their mean size goes down to 4 nm.<sup>11,12</sup> This observation leads to an interesting point about the lower limit down to which the DF amplitude decreases. Simulations carried out under density functional theory formalism showed that the key quantity in controlling the dielectric properties is given by the number of Si QDs.<sup>27-31</sup> Hence, for a free-standing 239-atom (2.2 nm in diameter) Si cluster passivated by H atoms, Weissker *et al.*<sup>27-29</sup> deduced  $A \approx 6$ . In the case of embedded Si nanoparticles, they computed  $A \approx 20$ , also for an identical cluster. These reports revealed a distribution of oscillator strengths to high photon energy above 3.5 eV. As described previously, in our case the DF amplitude is drastically reduced, as can be seen in Fig. 4. For example, the amplitude  $A$  varies from 37.5 to 9.49 when  $\sigma$  changes from 1 to 1.4. All values are summarized in Table I. Thus, our computations support the idea of an influence of the SD in order to explain the differences between the DF line shapes as observed in Fig. 3 and Table II.

Next we focus on the broadening  $C$  of the DF line shape. It is known that the broadening may result, on one hand, from either the radiative pair recombination or the scattering of the electron-hole pair with impurities in the nanocrystal (homogeneous broadening). On the other hand such broadening may also be owed to the presence in the SRSO film of a significant number of Si QDs with different sizes (inhomogeneous broadening).<sup>22</sup> Besides, Alonso *et al.*<sup>14</sup> attributed the increasing broadening of the DF spectra to the growing number

of possible transitions. When performing ellipsometry characterization, the measurement is more likely to be inherently sensitive to the effect of inhomogeneous broadening. The broadening  $C$  of the imaginary DF is linked to the value of the full width at half maximum of the absorption peak. As could be expected, Table I shows that the effect of size dispersion is more stressed on the broadening than on the other parameters of the DF line shape. Indeed a 54.5% increase of  $C$  is noticed when  $\sigma$  is changed from 1.05 to 1.25. For  $\sigma \geq 1.30$  the full width at half maximum is beyond our experimental measurement range, and the corresponding value is not displayed. Table II displays that the values of  $C$  associated to the critical points of the line shape are enlarged in comparison with bulk Si. Notwithstanding, Table II suggests that  $C$  is rather subjected to notable modifications from one sample (work) to another. As a matter of fact, from the parameters presented in their paper, it can be noticed that Losurdo *et al.*<sup>9</sup> obtained a broadening close to 3.1 eV, much larger than that of amorphous Si. The same comment may hold when trying to match the results derived for the main transition of 4.0 ( $C \approx 1.32$ ) and 4.7 ( $C \approx 1.98$ ) nm Si-ncs, studied in Refs. 11 and 14. An enhancement of the broadening should be expected as the mean size of the Si nanoclusters diminishes. The outcome of these observations is that size dispersion may be at the origin of such differences, as emphasized by our results related to the variation of  $C$  with  $\sigma$  in Table I.

Third, theoretical calculations generally demonstrated that a shift toward higher energies of the whole DF line shape is expected for smaller Si QDs as far as quantum confinement is involved.<sup>27-31</sup> However, it is noteworthy to point out that in such reports the effects of SD were not taken into account. On an experimental point of view, the redshift of the main transition energy of the nanocrystalline Si DF, with respect to the  $E_2$  transition of c-Si, was noticed. This behavior was obtained in most of the preceding works employing ellipsometry modeling.<sup>9-13,32</sup> Particularly in Ref. 32, the DF obtained from the classical MG formula shows no blueshift of  $E$  but rather a redshift of approximately 0.1 eV with respect to the  $E_2$  position of c-Si. Nonetheless the calculations, based on ellipsometric data, we have undertaken (see Table I) reveal a significant blueshift of the transition energy  $E$  from 4.15 eV ( $\sigma = 1.00$ ) to 4.65 eV ( $\sigma = 1.20$ ). Gallas *et al.*<sup>11,12</sup> found a perceptible decrease of the magnitude of the  $E_1$ -like transition as the size of the Si QDs was reduced from 4 to 2.5 nm. They attributed this change to a transfer of the oscillator strength to higher energy states. However, in their paper, the authors detected no blueshift of the  $E_2$ -like peak, though they recognized that this behavior may come from the omission in the modeling of an inhomogeneous broadening owing to the size dispersion of the Si-ncs. As far as we are concerned our results in Table I stress on the fact that an accurate determination of the size dispersion may generate an appreciable modification of the transition energy.

In addition, as evidenced in prior studies,<sup>3-7</sup> a strong correlation exists between the band gap energy and the other parameters (amplitude, broadening and transition energy) of the DF line shape. Hence an under/overestimation of one of the latter quantities may alter in a noticeable way the evaluation of the gap energy. Delley and Steigmeier<sup>38</sup> applied density functional approach to calculate the electronic structure and

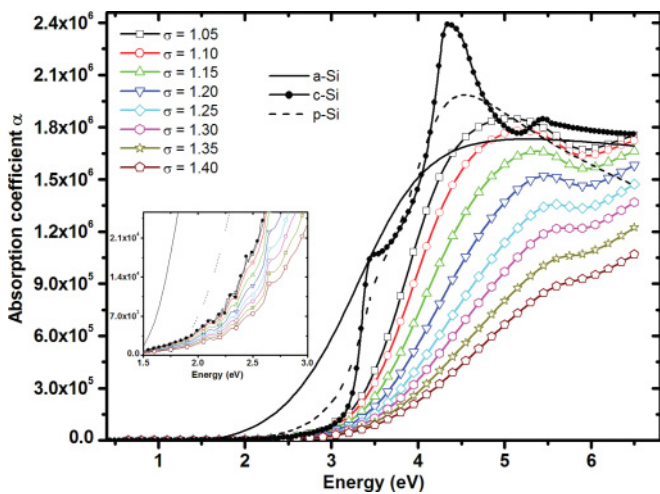


FIG. 5. (Color online) Influence of size dispersion on the absorption coefficient line shape for different values of the size dispersion  $\sigma$ . The absorption coefficient of amorphous, crystalline and polycrystalline silicon are also represented. The inset shows the absorption edge between [1.5–3.0 eV].

band gap of finite (up to 750 atoms or 3-nm-sized) Si structures. They showed that the band gap  $E_g$  scales linearly as  $(2 \cdot R)^{-1}$ . Contrary to the previous authors Ögüt *et al.*<sup>39</sup> took into account the size dependence of the self-energy correction in their first principles simulations. They computed the optical gaps of spherical Si clusters with diameters up to 2.7 nm and assessed a  $(2 \cdot R)^{-0.7}$  dependence. Experimentally, Nguyen *et al.*<sup>40</sup> measured by *in situ* spectroscopic ellipsometry the dielectric properties of ultrathin crystalline Si films. In that report the investigated films varied between 0.6 to 1.3 nm. They obtained a linear increase of the gap energy—from 2.75 to 3.0 eV—as the layer gets thinner. The dependence between band-gap energy and size dispersion can be evidenced by examining the absorption coefficient  $\alpha(E)$  spectra. In this manner Fig. 5 describes the evolution of the  $\alpha(E)$  of Si QDs as the size dispersion  $\sigma$  is raised. The absorption coefficient is directly deduced from the real and imaginary DF. The line shapes of  $\alpha(E)$  are also plotted for amorphous (a-Si), crystalline and polycrystalline (p-Si) silicon for comparison. Up to 3 eV the absorption coefficient of the Si QDs is rather close to that of c-Si. Above 3 eV the Si QDs' absorption is obviously amorphous-like, and the influence of size dispersion starts to be more stressed. Similarly to the evolution of the dielectric response of the Si QDs, the increase of  $\sigma$  progressively moves the absorption peak forward higher energies. Meanwhile the broadening that is induced by such elevation of  $\sigma$  increasingly smears the absorption peak. In some works the Si QDs' gap energy  $E_g^{\text{Tauc}}$  was deduced from a Tauc representation. This method consists in the extrapolation of the linear domain of the curve  $(\alpha \times E)^{1/2}$ .<sup>10,14</sup> However such a method of determination of  $E_g^{\text{Tauc}}$  value has to be handled with care. Indeed it is well known that as  $k(E)$  is close to zero, ellipsometry measurements may be tainted with uncertainties. For this reason we have evaluated only the optical gap  $E^{04}$ , which is defined as the photon energy at which  $\alpha = 10^4 \text{ cm}^{-1}$ , as done by Gallas *et al.*<sup>11,12</sup> Figures 4 and 5 and Table I reveal that  $E^{04}$  increases from 2.28 eV ( $\sigma = 1.05$ ) to 2.61 eV ( $\sigma = 1.40$ ). These  $E^{04}$  values are significantly higher than that of

a-Si ( $E^{04} = 1.68 \text{ eV}$ ) or p-Si ( $E^{04} = 1.91 \text{ eV}$ ). Nonetheless they remain close to the  $E^{04}$  of c-Si (2.27 eV) for relatively low  $\sigma$ . Accordingly, as  $\sigma$  is raised the blue shift of the absorption edge may primarily be attributable to the greater contribution of smaller sizes. However, as depicted in Table II, these former theoretical predictions do not every time comply with the trend observed from experimental results on Si QDs. In fact, an expansion of  $R$  from 1.5<sup>9</sup> to 2.35 nm<sup>14</sup> does not induce a systematic reduction of  $E_g$ , even though the latter quantity is blueshifted in comparison with the gap energy of bulk crystalline Si. Furthermore, a significant difference of 0.35 eV resides in the  $E_g$  values of Si-ncs with 4.6 nm<sup>10</sup> and 4.7 nm<sup>14</sup> average sizes (see Table II). Hence, as shown in Table I, the incorporation of an SD into the modeling should bring some meaningful corrections to the estimation of  $E_g$ . In regard to the evaluation of the nature of the band gap an open subject remains. Delley and Steigmeier found a direct band gap.<sup>38</sup> Our results tend to convey an indirect-like gap for Si QDs. On this point, former results deduced from ellipsometry modeling seem to conform with our deduction.<sup>14,40</sup>

Fifth, concerning previous ellipsometric modeling only little attention has been paid to the analysis of the static dielectric constant  $\epsilon_0$  (or real part of the low frequency DF) with size. The precise determination of  $\epsilon_0$  may be of particular importance in the conception of electronic devices.<sup>10,34</sup> We will subsequently show that theoretical calculations also demonstrate such a reduction of  $\epsilon_0$ . Nonetheless, Ng *et al.*<sup>41</sup> determined  $\epsilon_0$  for 4.5-nm-sized Si-ncs embedded in SiO<sub>2</sub>. They showed that  $\epsilon_0$  for nanocrystalline Si dots are significantly reduced  $\epsilon_0 = 9.8$  in comparison to the bulk one. Their result was thoroughly supported by C-V measurements.<sup>41</sup> Our results denote that the static dielectric constant  $\epsilon_0$  is affected by an increase in the size dispersion also. This is evidenced by the modification of  $\epsilon_r$  at 0.65 eV for various  $\sigma$ , as shown in the inset of Fig. 4. Actually  $\epsilon_0$  is split by nearly a factor of 1.23 when  $\sigma$  rises from 1.00 to 1.20. However, contradictory values for the evolution of  $\epsilon_0$  are presented in the literature. Indeed  $\epsilon_r$  is divided by more than 3, though Si-ncs with approximately the same size were investigated, depending on whether the work of Gallas *et al.*<sup>11</sup> or Alonso *et al.*<sup>14</sup> is considered. Furthermore, it is shown in the same Table II that a 2% difference in the average size of the Si-ncs could lead up to a discrepancy of 41% in the evaluation of their corresponding  $\epsilon_0$ .<sup>10,14</sup> In this regard our results explain such deviations in terms of size dispersion.

Until now in this paper, we have proceeded with a scrupulous examination of the main published data regarding the parameters that influence directly the line shape of the optical function of Si nanoclusters. We have identified five important parameters: amplitude  $A$  of  $\epsilon_i$  and associated broadening  $C$ ; transition energy  $E$  and optical gap  $E^{04}$ . The plot of  $\epsilon_r$  has been used to extract the static dielectric constant  $\epsilon_0$ . The quantitative evolution of such parameters versus the size dispersion  $\sigma$  is illustrated in Fig. 6. Again, the dependence of the DF parameters with SD is shown for a realistic variation of  $\sigma$  between 1.05 and 1.20. It has been noted that annealing of SRSO samples at high temperatures (at least 1000 °C) leads to the formation of Si QDs with standard deviations that generally vary around  $\sigma = 1.20$ . This value of  $\sigma$  is reasonable because even much higher figures ( $\sigma \approx 1.40$ – $1.50$ ) were obtained in a

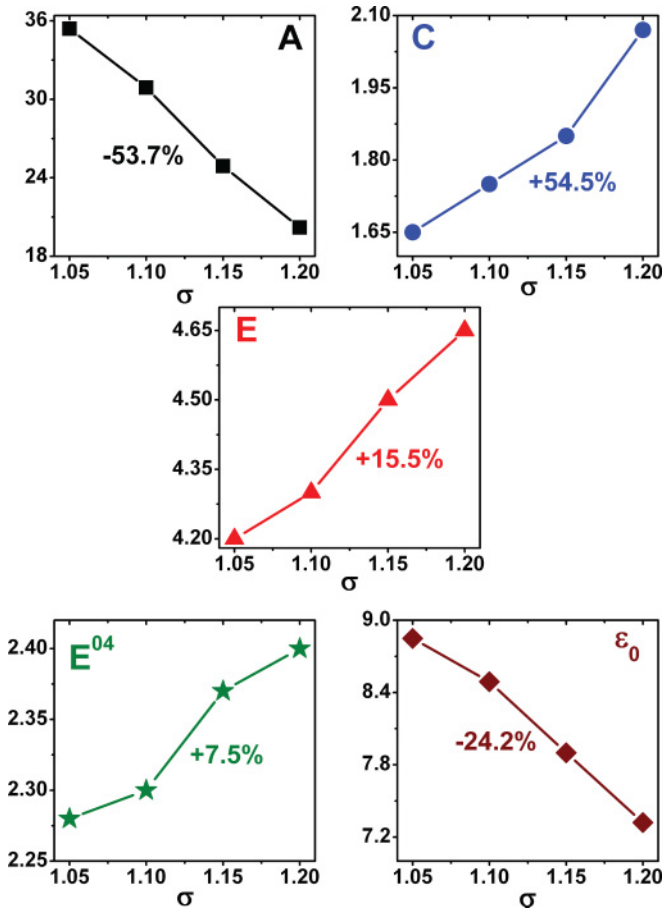


FIG. 6. (Color online) Illustration of the quantitative evolution of the parameters that determine the line shape of the DF versus the size dispersion  $\sigma$ . The figured parameters are the amplitude  $A$ , the broadening  $C$ , the transition energy  $E$ , the optical gap  $E^{04}$ , and the static dielectric constant  $\varepsilon_0$ .

prior research.<sup>20</sup> It should be noted that SD deduced from TEM analysis represents local information on the sample. When ellipsometry experiment is undertaken, the light beam probes several  $\mu\text{m}^2$  up to  $\text{mm}^2$  of the sample surface. Consequently, the effect of SD should be emphasized on the ellipsometry measurement. This observation has revealed to us rather convincing arguments showing that SD, as highlighted in electron microscopy observations, should be taken into account in the ellipsometric modeling via the MMG formulation (see Eq. (6) and Ref. 22). Thus, we have first determined the dielectric response as a function of SD in spectral range from 0.6 to 6.5 eV (see Figs. 4 and 5), and now we shall investigate on its effect on the parameters describing the size dependence of the low frequency static dielectric constant of Si nanostructures.

#### IV. SD IMPACT ON THE STATIC DIELECTRIC CONSTANT AFFECTED BY QUANTUM CONFINEMENT AND SURFACE POLARIZATION

Theoretical works have focused, likewise, on the evaluation of the low frequency static dielectric constant for Si nanostructures. In this manner, Wang and Zunger evaluated, by quantum mechanical pseudopotential simulations,  $\varepsilon_0$  for Si QDs with an average radius between 0.8 and 2 nm. They

showed that  $\varepsilon_0$  is importantly decreased relatively to the bulk value.<sup>42,43</sup> Apart from that previous report, Delerue *et al.*<sup>44</sup> employed tight-binding simulations in order to evaluate the effective dielectric constant of nanostructured Si layers. In order to explain the reduction of  $\varepsilon_0$  with size, two competing physical mechanisms have been put forward hitherto. On one hand the first mechanism may be owed to the opening of the band gap or in other words to QCE. It has been shown in previous studies that QCE affects the static dielectric constant with a size dependence that is expressed as:<sup>39,40,42,43</sup>

$$\varepsilon_0^{\text{QCE}}(R) = 1 + \frac{\varepsilon_0^{\text{bulk}} - 1}{1 + (\alpha/R)^l}, \quad (9)$$

where  $\varepsilon_0^{\text{bulk}} = \varepsilon_0^{\text{c-Si}} = 11.95$  is the dielectric constant of the bulk material taken here at photon energy of 0.65 eV.<sup>27–29</sup>  $(\alpha, l)$  is a pair of variable parameters, which are used to fit the dependence of  $\varepsilon_0$  with the mean radius of the Si nanostructures. The  $(\alpha, l)$  parameters depend on the size and shape of the Si nanostructures. Wang and Zunger,<sup>42</sup> Delerue and Allan,<sup>44</sup> and Ögüt *et al.*<sup>39</sup> assigned to this pair the values (0.425, 1.25), (1.84, 1.18), and (0.97, 1.3), respectively. According to the literature, the  $l$  exponent lies between 1 and 2. The size parameter  $\alpha$  has to be less than the QD mean radius  $\bar{R}$  when a strong confinement regime applies to the system.<sup>42</sup> The smaller the  $\alpha/R$  ratio is, the more intense the confinement regime becomes.<sup>42</sup> On the other hand the second mechanism at the origin of the diminution of  $\varepsilon_0$  may come from the breaking of polarizable bonds.<sup>44–47</sup> It is also referred to as surface polarization effect (SPE). It has been established that SPE influences the static dielectric constant with a size dependence that is quite different from QCE and formulated as

$$\varepsilon_0^{\text{SPE}}(R) = \varepsilon_0^{\text{bulk}} - (\varepsilon_0^{\text{bulk}} - \varepsilon_{\text{surface}}) \cdot \frac{d_{\text{surface}}}{R} = \varepsilon_0^{\text{bulk}} - \frac{s^{\text{SPE}}}{R}, \quad (10)$$

where  $d_{\text{surface}}$  (in nm) is the thickness of the surface shell,  $\varepsilon_{\text{surface}}$  is its corresponding DF, and  $s^{\text{SPE}}$  is defined as<sup>47</sup>

$$s^{\text{SPE}} = (\varepsilon_0^{\text{bulk}} - \varepsilon_{\text{surface}}) \cdot d_{\text{surface}}. \quad (11)$$

Recently, Yoo and Fauchet made use of spectroscopic ellipsometry in order to determine the dielectric constant, at 0.73 eV, of Si nanoslabs of various thicknesses from 3.2 to 13.1 nm.<sup>47</sup> They noticed that when  $l = 1$  and  $\alpha/R \ll 1$ , then the effects of QCE and SPE become quite similar at the first order.<sup>47</sup> In fact, Eq. (9) can be approximated to

$$\varepsilon_0^{\text{QCE}}(R) \approx \varepsilon_0^{\text{bulk}} - \frac{s^{\text{QCE}}}{R}, \quad (12)$$

where

$$s^{\text{QCE}} = (\varepsilon_0^{\text{bulk}} - 1) \cdot \alpha. \quad (13)$$

Now let us consider the size-dependent expressions of  $\varepsilon_0$  given by Eqs. (9) and (10). We expect that these latter relationships are not only valid for the average radius of the Si QDs, but they remain well founded for each QD radius with a given size comprised within the SD  $P(R)$ . Next, by inputting the expressions of  $\varepsilon_0^{\text{QCE}}(R)$  and  $\varepsilon_0^{\text{SPE}}(R)$  into Eq. (6), for  $E = 0.65$  eV we can numerically solve it. Afterward, the parameters  $(\alpha, l)$  and  $(d_{\text{surface}}, \varepsilon_{\text{surface}})$  can be extracted. The



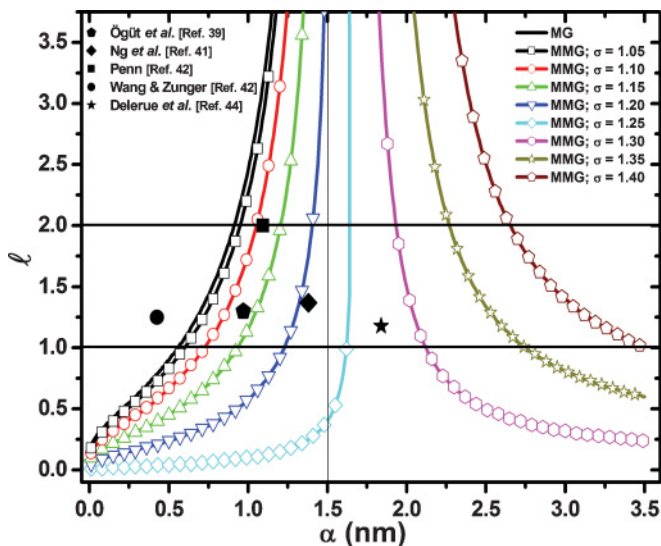


FIG. 7. (Color online) Values of the  $(\alpha, l)$  parameters that fit with the modeled effective dielectric constant  $\epsilon_0^{\text{eff}} = 2.269$  at 0.65 eV obtained by considering the influence of quantum confinement on the static dielectric constant  $\epsilon_0^{\text{QCE}}(R)$ . The horizontal dotted lines at  $l = 1$  and  $l = 2$  define the region where the values of  $l$  should lie (as observed in the literature).

value of the effective dielectric constant is deduced from the  $\lambda$ -by- $\lambda$  inversion and is such that  $\epsilon_0^{\text{eff}} = 2.269$ .<sup>33</sup> Moreover, at  $E = 0.65$  eV the dielectric constant of the silica matrix is given by  $\epsilon_0^{\text{SiO}_2} = 2.071$ .<sup>23</sup>

Figure 7 shows the  $(\alpha, l)$  values obtained from numerical integration of the MMG formula given by Eq. (6). We point out that the  $(\alpha, l)$  provided in this figure are determined from experimental data only. Contrary to the referenced  $(\alpha, l)$  extracted from the literature, we obtain in Fig. 7 not single points—as in Refs. 39, 42, and 44—but curves, because our study deals only with one sample characterized by a unique average size. In case of the consideration of other samples with different mean size, we could remove the uncertainty about the exact value of the couple  $(\alpha, l)$ . Hence, according to the literature data we will focus on solutions for which  $l$  lies between 1 and 2. It is seen in Fig. 7 that the consideration of a specific value of  $\sigma$  results in a different  $l = f(\alpha)$  curve. Subsequently, it can be deduced that the static dielectric constant of the Si QDs is affected by the SD effect. As far as  $\sigma$  remains small ( $\sigma < 1.05$ ), the  $(\alpha, l)$  points obtained using MG are close to those derived with MMG. It is observed that for  $\sigma = 1.20$ , for the SRSO sample examined in this study,  $\alpha$  varies around 1.30, near  $\bar{R} = 1.50$  nm. This could suggest an intermediate confinement regime, which is in good agreement with the rather flat PL peak observed at room temperature.<sup>32</sup> For higher values of the size standard deviation, the associated  $\alpha$  is larger, which could signify much lower confinement.

Figure 8 depicts the evolution of  $\epsilon_{\text{surface}}$  versus  $d_{\text{surface}}$ . The result that is transmitted across this figure is that size dispersion  $\sigma$  affects the evolution of the parameters  $(d_{\text{surface}}, \epsilon_{\text{surface}})$ . For a given  $\sigma$ ,  $\epsilon_{\text{surface}}$  asymptotically grows with  $d_{\text{surface}}$ . The larger  $\sigma$  is, the lower the value of  $\epsilon_{\text{surface}}$  becomes. In addition the lessening of  $\epsilon_{\text{surface}}$  is more important for a thinner surface region. Besides, in Fig. 8 the variation of  $\epsilon_{\text{surface}}$  versus  $d_{\text{surface}}$

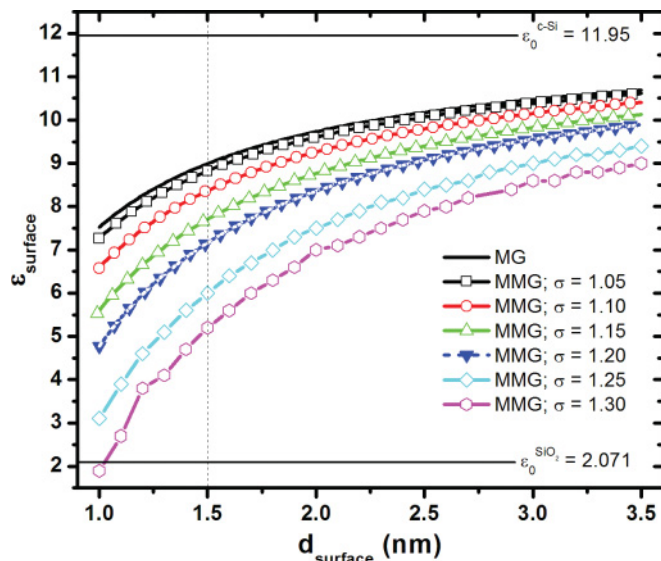


FIG. 8. (Color online) Values of the  $(d_{\text{surface}}, \epsilon_{\text{surface}})$  parameters that fit with the modeled effective dielectric constant  $\epsilon_0^{\text{eff}} = 2.269$  at 0.65 eV obtained by considering the effect of surface polarization on the static dielectric constant  $\epsilon_0^{\text{SPE}}(R)$ . The vertical dotted line at  $d_{\text{surface}} = 1.5$  nm is given as a comparison to the value of the average radius ( $\bar{R} = 1.5$  nm) of the Si QDs.

may recall that of the dielectric constant versus the silicon sphere radius as presented in Fig. 2 of Ref. 43.

Table III shows the evolution of  $\alpha$  and  $\epsilon_{\text{surface}}$  with  $\sigma$  for  $l = 1$  and  $d_{\text{surface}} = \bar{R} = 1.5$  nm. The values of  $\alpha$  and  $\epsilon_{\text{surface}}$  were deduced from Figs. 7 and 8. The  $s^{\text{SPE}}$  quantity defined by Eq. (11) remains almost constant for a fixed value of  $\sigma$ : indeed it is approximately equal to 4.4 for MG ( $\sigma = 1.00$ ), and it successively goes up to 4.7 for  $\sigma = 1.05$  to 10.1 for  $\sigma = 1.30$ . As a comparison we recall that Yoo and Fauchet<sup>47</sup> obtained more or less  $s \approx 6.6$  for Si nanoslabs with a 0.5-nm-thick surface roughness layer. Table III shows that for a 1.5-nm-thick surface region,  $\epsilon_{\text{surface}}$  reaches approximately the same value as  $\epsilon_0$ , as determined in Table I. However, a slight increase of the relative difference between  $\epsilon_{\text{surface}}$  and  $\epsilon_0$  is observed as  $\sigma$  goes up. This gap comes from the fact that the influence of size was implicitly assumed in the determination of  $\epsilon_0$  in Table I. Conversely, it is observed in Table III that the values of  $s^{\text{QCE}}$  are much higher than those of  $s^{\text{SPE}}$ . This is owed to the

TABLE III. Influence of the standard deviation  $\sigma$  on the  $(\alpha, l)$ ,  $(d_{\text{surface}}, \epsilon_{\text{surface}})$ ,  $s^{\text{QCE}}$ , and  $s^{\text{SPE}}$  parameters assigned to describe the influence of quantum confinement and surface polarization on the size-dependent static dielectric constant at 0.65 eV. The definition of the other parameters is provided in the text.

$\sigma$	Quantum confinement			Surface polarization		
	$\alpha$ (nm)	$l$	$s^{\text{QCE}}$	$\epsilon_{\text{surface}}$	$d_{\text{surface}}$ (nm)	$s^{\text{SPE}}$
1.00	0.55		6.02	8.99		4.44
1.05	0.60		6.57	8.82		4.69
1.10	0.72	1.00	7.88	8.37	1.50	5.37
1.15	0.93		10.18	7.71		6.36
1.20	1.22		13.36	7.16		7.18

large values of  $\alpha$ , which leads to a relaxation of the condition  $\alpha/R \ll 1$  in our investigated film.

Previously, some works more or less supported the idea that the static dielectric constant is not affected by a possible broadening of the electronic transition resonances near the  $E_1$ -like and  $E_2$ -like structures of c-Si.<sup>14,41,46</sup> Our results do not categorically allow having a definite opinion on whether the reduction of  $\epsilon_0$  is mainly attributable to surface polarization or quantum confinement. Nonetheless, we have shown that both mechanisms come into play. Furthermore, we have stressed here on the fact that inhomogeneous broadening does substantially influence the value of  $\epsilon_0$ . Certainly a slight increase of the size dispersion should lead to significant variations of the characteristic parameters describing QCE and SPE. On that account, a conspicuous fall, more than expected, of the static dielectric constant is likely to occur as the influence of size dispersion is considered.

## V. CONCLUSIONS

This paper deals with the insertion of an SD in the modeling of the optical properties of nanoscale Si when using spectroscopic ellipsometry characterization. To date only a single average size has been implicitly considered in the modeling. We have shown that such assumption has led to some uncertainties. This observation has been evidenced by a comparative study of the various results presented in the

literature. Therefore, we have presented an MMG formula. This mixture model takes into account explicitly the effect of SD on the optical response of Si nanoclusters embedded in a dielectric (silica) matrix. The ellipsometric computations we have undertaken and that were performed without using any parameterized dispersion formula have shown that the three parameters  $f$  (their volume fraction),  $\bar{R}$  (their average radius), and  $\sigma$  (their dispersion in size) are interrelated. Hence the influence of one of these parameters cannot be investigated while disregarding the effect of the two others. The results infer strong evidence that  $\sigma$  plays a non-negligible role in the evolution of the whole line shape of the DF. In fact it smears the peaks associated to the  $E_1$ -like and  $E_2$ -like transitions; it sensitively reduces their corresponding amplitudes and slightly contributes to a blueshift of both the optical gap onset and the absorption peaks. Additionally it has been shown that, owing to inhomogeneous broadening, the low frequency dielectric constant of Si nanostructures is not independent of SD.

## ACKNOWLEDGMENTS

We thank Laurent Broch from LPMD, Christian Louis from Horiba Jobin Yvon, Inc., and Martin Michael Müller from the Laboratoire de Physique Moléculaire et Collisions (Université Paul Verlaine-Metz) for their interest in this work and for providing the authors with appreciable advice in the MATHEMATICA calculation.

\*alsaleh.keita@univ-metz.fr

<sup>1</sup>P. Yu and M. Cardona, *Fundamentals of Semiconductors*, 4th ed. (Springer-Verlag, Berlin, 2010), Chap. 6, pp. 254 and 264.

<sup>2</sup>D. E. Aspnes and A. A. Studna, *Phys. Rev. B* **27**, 985 (1983).

<sup>3</sup>A. R. Forouhi and I. Bloomer, *Phys. Rev. B* **38**, 1865 (1988).

<sup>4</sup>S. Adachi, *Phys. Rev. B* **38**, 12966 (1988).

<sup>5</sup>G. E. Jellison Jr., M. F. Chisholm, and S. M. Gorbalkin, *Appl. Phys. Lett.* **62**, 3348 (1993).

<sup>6</sup>G. E. Jellison Jr. and F. A. Modine, *Appl. Phys. Lett.* **69**, 371 (1996).

<sup>7</sup>G. E. Jellison, Jr. and F. A. Modine, *Appl. Phys. Lett.* **69**, 2137 (1996).

<sup>8</sup>L. Pavesi, L. Dal Negro, C. Mazzeloni, G. Franzò, and F. Priolo, *Nature* **408**, 440 (2000) and Fig. 3 in the Supplementary Information.

<sup>9</sup>M. Losurdo, M. M. Griangregorio, P. Capezutto, G. Bruno, M. F. Cerqueira, E. Alves, and M. Stepikhova, *Appl. Phys. Lett.* **82**, 2993 (2003).

<sup>10</sup>L. Ding, T. P. Chen, Y. Liu, M. Yang, J. I. Yong, Y. C. Liu, A. D. Trigg, F. R. Zhu, M. C. Tan, and S. Fung, *J. Appl. Phys.* **101**, 103525 (2007).

<sup>11</sup>I. Stenger, B. Gallas, L. Siozade, C.-C. Kao, S. Chenot, S. Fisson, G. Vuye, and J. Rivory, *J. Appl. Phys.* **103**, 114303 (2008).

<sup>12</sup>B. Gallas, I. Stenger, C.-C. Kao, S. Fisson, G. Vuye, and J. Rivory, *Phys. Rev. B* **72**, 155319 (2005).

<sup>13</sup>R. J. Zhang, Y. M. Chen, W. L. Lu, Q. Y. Cai, Y. X. Zheng, L. Y. Chen, *Appl. Phys. Lett.* **95**, 161109 (2009).

<sup>14</sup>M. I. Alonso, I. C. Marcus, M. Garriga, A. R. Goñi, J. Jedrzejewski, and I. Balberg, *Phys. Rev. B* **82**, 045302 (2010).

<sup>15</sup>A. Sa'ar, *J. Nanophotonics* **3**, 032501 (2009).

<sup>16</sup>W. Lamb, D. M. Wood, and N. W. Ashcroft, *Phys. Rev. B* **21**, 2248 (1980).

<sup>17</sup>D. E. Aspnes, *Am. J. Phys.* **50**, 704 (1982).

<sup>18</sup>W.-Y. Wu, J. N. Schulman, T. Y. Hsu, and Uzi Efron, *Appl. Phys. Lett.* **51**, 710 (1987).

<sup>19</sup>V. V. Nikolaev and N. S. Averkiev, *Appl. Phys. Lett.* **95**, 263107 (2009).

<sup>20</sup>R. Espiau de Lamaestre and H. Bernas, *Phys. Rev. B* **73**, 125317 (2006).

<sup>21</sup>V. A. Belyakov, V. A. Burdov, R. Lockwood, and A. Meldrum, *Adv. Optical Tech.* **2008**, 279502 (2008).

<sup>22</sup>L. Bányai and S. W. Koch, *Semiconductor Quantum Dots* (World Scientific, Singapore, 1993), Chap. 2, pp. 20–29.

<sup>23</sup>L. Fu, P. B. Macedo, and L. Resca, *Phys. Rev. B* **47**, 13818 (1993).

<sup>24</sup>A. V. Goncharenko, V. Z. Lozovski, and E. F. Venger, *J. Phys.: Condens. Matter* **13**, 8217 (2001).

<sup>25</sup>M. Gilliot, A. En Naciri, L. Johann, J. P. Stoquert, J. J. Grob, and D. Muller, *Phys. Rev. B* **76**, 045424 (2007).

<sup>26</sup>R. W. Collins and A. S. Ferlauto, in *Handbook of Ellipsometry*, edited by H. G. Tompkins and E. A. Irene (William Andrew, Norwich, NY, 2005), Chap. 2, pp. 137 and 178.

<sup>27</sup>H.-C. Weissker, J. Furthmüller, and F. Bechstedt, *Phys. Rev. B* **67**, 165322 (2003).

<sup>28</sup>H.-C. Weissker, J. Furthmüller, and F. Bechstedt, *Phys. Rev. B* **65**, 155327 (2002).

<sup>29</sup>H.-C. Weissker, J. Furthmüller, and F. Bechstedt, *Phys. Rev. B* **65**, 155328 (2002).

<sup>30</sup>L. E. Ramos, J. Paier, G. Kresse, and F. Bechstedt, *Phys. Rev. B* **78**, 195423 (2008).

- <sup>31</sup>K. Seino, F. Bechstedt, and P. Kroll, *Nanotechnology* **20**, 135702 (2009).
- <sup>32</sup>A. En Naciri, M. Mansour, L. Johann, J.-J. Grob, and J. Stoquert, *J. Chem. Phys.* **129**, 184701 (2008).
- <sup>33</sup>*Handbook of Optical Constants of Solids*, Edited by E. D. Palik, (Academic, Orlando, FL, 1985), Vol. 1, pp. 552 and 571.
- <sup>34</sup>D. M. Wood and N. W. Ashcroft, *Phys. Rev. B* **25**, 6255 (1982).
- <sup>35</sup>J. B. Khurgin, E. W. Forsythe, G. S. Tompa, and B. A. Khan, *Appl. Phys. Lett.* **69**, 1241 (1996).
- <sup>36</sup>L. D. Landau, E. M. Lifshitz, and L. P. Pitaevskii, *Electrodynamics of Continuous Media*, 2nd ed. (Butterworth-Heinemann, Oxford, 1984), Chap. 9, p. 282.
- <sup>37</sup>F. Wooten, *Optical Properties of Solids* (Academic Press, New York, 1972), Chap. 3, pp. 46 and 72.
- <sup>38</sup>B. Delley and E. F. Steigmeier, *Phys. Rev. B* **47**, 1397 (1993).
- <sup>39</sup>S. Ögüt, J. R. Chelikowsky, and S. G. Louie, *Phys. Rev. Lett.* **79**, 1770 (1997).
- <sup>40</sup>H. V. Nguyen, Y. Lu, S. Kim, M. Wakagi, and R. W. Collins, *Phys. Rev. Lett.* **74**, 3880 (1995).
- <sup>41</sup>C. Y. Ng, T. P. Chen, L. Ding, Y. Liu, M. S. Tse, S. Fung, and Z. L. Dong, *Appl. Phys. Lett.* **88**, 063103 (2006).
- <sup>42</sup>L.-W. Wang and A. Zunger, *Phys. Rev. Lett.* **73**, 1039 (1994).
- <sup>43</sup>R. Tsu, D. Babić, and L. Ioriatti Jr., *J. Appl. Phys.* **82**, 1327 (1997).
- <sup>44</sup>C. Delerue and G. Allan, *Appl. Phys. Lett.* **88**, 173117 (2006).
- <sup>45</sup>X. Cartoixa and L.-W. Wang, *Phys. Rev. Lett.* **94**, 236804 (2005).
- <sup>46</sup>F. Trani, D. Ninno, and G. Iadonisi, *Phys. Rev. B* **75**, 033312 (2007).
- <sup>47</sup>H. G. Yoo and P. M. Fauchet, *Phys. Rev. B* **77**, 115355 (2008).